RESEARCH PAPER

Investigation of magnetic active core sizes and hydrodynamic diameters of a magnetically fractionated ferrofluid

Markus Büttner · Peter Weber · Frank Schmidl · Paul Seidel ·
Michael Röder · Matthias Schnabelrauch · Kerstin Wagner ·
Peter Görnert · Gunnar Glöckl · Werner Weitschies

Abstract In this work we address the question which relates between the size of the magnetically active core of magnetic nanoparticles (MNPs) and the size of the overall particle in the solution (the so-called hydrodynamic diameter d_{hyd}) exists. For this purpose we use two methods of examination that can deliver conclusions about the properties of MNP which are not accessible with normal microscopy. On the one hand, we use temperature dependent magnetorelaxation (TMRX) method, which enables direct access to the energy barrier distribution and by using additional hysteresis loop measurements can provide details about the size of the magnetically active cores. On the other hand, to determine the size of the overall particle in the solution, we use the magnetooptical relaxation of ferrofluids (MORFF) method, where the stimulation is done magnetically while the reading of the relaxation signal, however, is done optically. As a basis for the examinations in this work we use a ferrofluid that was developed for medicinal purposes and which has been fractioned magnetically to obtain differently sized fractions of MNPs. The two values obtained through these methods for each fraction shows the success in fractioning the original solution. Therefore, one can conclude a direct correlation between the size of the magnetically active core and the size of the complete particle in the solution from the experimental results. To calculate the size of the magnetically active core we found a temperature dependent anisotropy constant which was taken into account for the calculations. Furthermore, we found relaxation signals at 18 K for all fractions in these TMRX measurements, which have their origin in other magnetic effects than the Néel relaxation.

M. Büttner · P. Weber · F. Schmidl · P. Seidel (✉)
Institute of Solid State Physics, Friedrich Schiller
Universität Jena, Helmholtzweg 5, 07743 Jena, Germany
e-mail: Paul.Seidel@uni-jena.de

M. Büttner
e-mail: p0bumr@uni-jena.de

M. Röder · M. Schnabelrauch · K. Wagner · P. Görnert
INNOVENT e.V., Prüssingstraße 27B, 07745 Jena,
Germany

G. Glöckl · W. Weitschies
Institute of Pharmacy, Biopharmaceutics &
Pharmaceutical Technology, Ernst-Moritz-Arndt
University of Greifswald, Friedrich-Ludwig-Jahn-Str. 17,
17487 Greifswald, Germany

Introduction

A lot of different properties of magnetic nanoparticles (MNPs) play an important role in using these particle systems. Besides the outer shape of the

particles, which is examined using microscopic measurements, one finds a lot of questions regarding the magnetic properties, e.g., the use with hyperthermia and drug targeting.

The magnetic properties of the particles are mainly defined by the magnetic active volume V_m of the cores. In contrast to microscopic procedures, which only provide information about the overall size of the particles and thus information about V_m and the significant so-called magnetic dead layer, temperature dependent magnetorelaxometry (TMRX) provides information about the size of magnetically active volumes by using a temperature dependent measurement of the energy barriers (Romanus et al. 2003).

For biomedical applications the overall size of the particles in the solution is important. One determines these hydrodynamic diameters d_{hyd} by applying stray light procedures (e.g., photon correlation spectroscopy (PCS)). In this work the hydrodynamic diameters are investigated by using the magnetooptical relaxation of ferrofluids (MORFF) method (Romanus et al. 2001). The correlation of the results of PCS and MORFF measurements has been established already (Romanus et al. 2002). For our examinations, we used a water-based ferrofluid with a core of iron oxide and a shell of carboxymethyl dextran (CMD) (pH = 5.5).

The iron oxide cores are consisting of a mixture of maghemite Fe_2O_3 (68%) and magnetite Fe_3O_4 (32%). The ferrofluid has been fractionated into seven fractions by using a magnetic fractionation method. In this work we calculate the particle diameter from the obtained results of the measurements of the energy barrier distributions with respect to the temperature dependence of the anisotropy. Then we compare the behaviour of the obtained core diameters with the hydrodynamic diameters obtained by using the MORFF method.

TMRX method

Theoretical aspects

A detailed description of the underlying theoretical models has been published elsewhere (Romanus et al. 2007). The Néel relaxation time t_N of MNPs with an anisotropy K and a volume V_m is given by the formula

$$t_N = t_0 \exp\left(\frac{KV_m}{k_B T}\right) \tag{1}$$

where t_0 means a constant with a duration of $\sim 10^{-9}$ s and k_B the Boltzmann constant. One should consider that K also depends on the temperature. The magnetization relaxation of a system of MNPs with an energy barrier density distribution $\rho(E)$ (after being magnetized in a weak external field for a finite time t_{mag}) can be described as (Berkov and Kötitz 1996; Romanus et al. 2003)

$$M(t) = k_B T \rho(E^{max}) \delta m(E^{max}) \ln\left(1 + \frac{t_{mag}}{t}\right). \tag{2}$$

In this case $\delta m(E)$ indicates the magnetization change caused by the relaxation of particles with an energy barrier E. (E^{max}) is given by (E^{max}) $\approx k_B T \ln(t_{mag}/t_0)$. Equation 2 can be reformulated as

$$M(t) = M_0 \cdot \log\left(1 + t_{mag}/t\right) \tag{3}$$

with

$$M_0 = kT \cdot \rho(E^{max}) \cdot \delta m(E^{max}). \tag{4}$$

That implies when measuring the magnetization relaxation for a given temperature T and magnetization time t_{mag} and fitting the procured dependence by the $\ln(1 + t_{mag}/t)$ law one can directly attain the energy barrier density $\rho(E)$ multiplied by the corresponding magnetization change $\delta m(E)$. In a system of single-domain particles $\rho(E)$ is equivalent to the number of particles N with an anisotropy energy $E = KV$; $\delta m(E)$ is proportional to the magnetic volume of the particles at energy E. For fixed particles the relaxation due to Brownian motion is suppressed and only Néel relaxation contributes to the relaxation signal.

Experimental methods

The set-up for TMRX measurements has been described in detail elsewhere (Romanus et al. 2003). In principle, the system consists of a second-order SQUID gradiometer working in an unshielded environment at helium temperature to measure the magnetic relaxation signal and Helmholtz coils to magnetize the sample. To extract the necessary information from our measurements, we have used Eqs. 3 and 4 to describe the time decay of the sample

magnetization $M(t)$ due to the Néel relaxation. Accordingly, the magnetic field B of the sample should have the following time dependence:

$$B(t) = B_{\text{offset}} + B_0 \ln\left(1 + \frac{t_{\text{mag}}}{t}\right) \quad (5)$$

where the offset term is arbitrary, since SQUIDs do not supply absolute values. The value of B_0 was fitted from the measured data using Eq. 5. B_0 is proportional to M_0. The factor between B_0 and M_0 is an apparatus constant. According to Eqs. 4 and 5 we calculated the values of $\rho(E^{\max}) \, \delta m(E^{\max})$ in arbitrary units. The samples are magnetized for 1 s using a magnetic flux density of 1 mT. After a deadtime of 20 ms the $B(t)$ data is recorded for 1 s with a sampling rate of 2 kHz. This procedure is continuously repeated at sample temperatures between liquid helium temperature and room temperature. The sample is situated in a special designed anticryostat to slowly cool down the sample. Figure 1 shows a schematic of the cryostat containing the low-T_C SQUID gradiometer as well as the sample in an anticryostat.

The sample temperature is measured using a miniature temperature sensor (silicon diode DT-420, Lake Shore Cryotronics) directly at the MNP-sample.

MORFF method

Theoretical aspects

Magnetic fluids become birefringent when a magnetic field is applied perpendicular to the axis of light impinging the fluid, as the MNP contained in the magnetic fluid tend to align in the direction of the external field (Cotton and Mouton 1907) (Cotton–Mouton effect). After switching off the magnetizing field one can observe a relaxation of the birefringence. This phenomenon is also called the magnetic field-induced transient birefringence. Assuming a Brownian relaxation mechanism of MNP in a ferrofluid the birefringence of the ferrofluid decays according to (Perrin 1934)

$$\Delta n = \Delta n_0 \, e^{-\frac{t}{\tau_B}} \quad (6)$$

with Δn_0 being the initial birefringence value and τ_B the Brownian relaxation time:
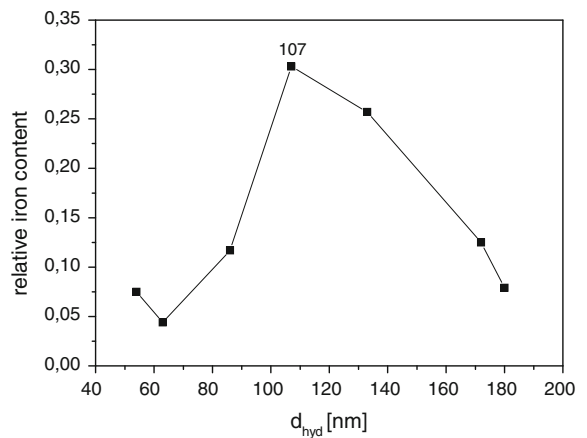
Fig. 1 Relative iron content and hydrodynamic diameter d_{hyd} of the fractionated samples

$$\tau_B = \frac{3\eta V_{\text{hyd}}}{kT}. \quad (7)$$

With known values for the viscosity η of the ferrofluid, the temperature T, Boltzmann's constant k and τ_B determined from the relaxation measurement it is possible to calculate the hydrodynamic volume V_{hyd} of the particles.

Measurement set-up

The measurement set-up for the determination of the MORFF consists of a laser, a polariser aligned orthogonal to an analyzer and at 45° to the magnetic field axis, a retardation plate with its slow axis parallel to the polariser, a cuvette containing the sample and a detector mounted on an optical bench. The cuvette is placed into a solenoid generating a pulsed magnetic field of 10 kA/m with a magnetization time of 10 ms. After switching off the magnetizing field the relaxation of the birefringence is recorded by a photo-diode (Romanus et al. 2001).

Low temperature measurement set-up

To gain information about the anisotropy of uniaxial particles, one can determine the magnetic coercivity at temperatures lower than the blocking temperature; if the easy axis is parallel to the applied field, then $H_C = H_K = 2K/M_S$ (H_K is the anisotropy field and M_S the saturation magnetization of the particles). The

coercivity is given by $H_C = 0.479H_K$ and the remanence is $M_R \approx 0.5M_S$ (ignoring the particle interaction) for a multi-particle system with uniaxial single-particle anisotropy and randomly oriented easy axes (Blums et al. 1997; Buschow 2005).

A commercial SQUID susceptometer (S600X, Cryogenic LTD, UK) was used to measure the magnetic properties. It is an ultra-sensitive instrument for DC and AC measurement of magnetic properties as a function of magnetic field and temperature. The SQUID sensor has an input noise power sensitivity of approximately 10^{-30} J $Hz^{-1/2}$. The instrument was operated in normal DC mode (measurement of the total magnetic moment was taken by moving the sample through a set of pick-up coils). A superconducting coil applied the magnetic field (up to 6 T). There is an adequately homogeneous field inside the coil. The sample temperature (1.6–370 K) is controlled by a helium gas flow cryostat.

Magnetic particles and sample preparation

For our examinations we use a ferrofluid developed by INNOVENT Jena for medical purposes. A description of the manufacturing of the ferrofluid has been published elsewhere in principle (Wagner et al. 2004).

It is a water-based ferrofluid (V190) with an iron oxide core and a CMD shell. The iron oxide contains iron(II) and iron(III)-ions representing a mixture of magnetite and maghemite. Based on the composition of both iron oxides, the oxide ratio in the particle cores was obtained after determining the concentration of the iron(II) and iron(III) ions by conventional titration. As shell material a CMD with a degree of carboxymethyl substituents per anhydroglucose unit (DS) of 0.7 was employed. The starting molecular weight of the dextran polymer was in a range between 15 and 20 kDa. The CMD content in the ferrofluid amounts to 13 mg/mL. According to the obtained iron ion concentrations after production, the magnetic solution contains 68% maghemite (saturation moment at 0 K = 76 emu/g and $\rho = 4.9$ g/cm^3) and 32% magnetite (saturation moment at 0 K = 98 emu/g and $\rho = 5.2$ g/cm^3). The initial solution of the ferrofluid with broad particle size distribution was fractionated by using a electromagnet (Bruker B-E 10v) with a variable coil current

Table 1 Detailed fractionation parameters and iron content (percentage of initial solution in %)

Fraction number	Coil current I_{Coil} (A)	Iron content (in % of the initial solution)
1	1.00	7.5
2	0.40	4.4
3	0.20	11.7
4	0.10	30.3
5	0.05	25.7
6	0.01	12.5
7	0.00	7.9

I_{Coil} and a magnetic separation column (MACS XS, Miltenyi Biotech). The fractionating does not influence the ratio between magnetite and maghemite in the particle core.

For the first fraction the coil current was set to 1 A and was reduced for further fractions accordingly. More details on the fractionation parameters can be found in Table 1.

Each sample was prepared for consecutive TMRX and hysteresis loop measurements. All samples contain 1 μmol Fe. To prevent interaction between the magnetic particles, the particles were homogeneously distributed in a volume of about 45 μL in sample holders made of Teflon. Then the samples were lyophilized in mannitol to immobilize the particles.

Measurement results and discussion

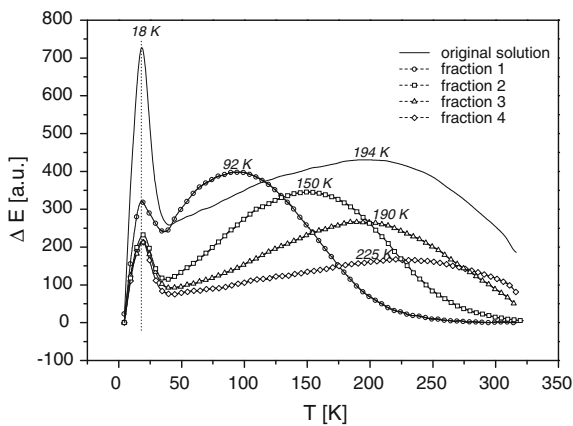### Results of the measurement of the hydrodynamic diameter of the samples

Table 2 shows the obtained results when determining the hydrodynamic diameter d_{hyd}.

The obtained hydrodynamic diameters of the different fractions provide clear indication for the success of the fractioning regarding the separation of particles according to their magnetic moment. Furthermore, one can extrapolate a direct connection between the core diameter and the hydrodynamic diameter.

To assess how the measured fractioned samples agree with the initial solution and to test the reliability of the measurement system, Fig. 1 shows

Table 2 Hydrodynamic diameter of the fractionated samples and the initial solution

Sample	d_{hyd} (nm)
Original solution	102
Fraction 1	54
Fraction 2	63
Fraction 3	86
Fraction 4	107
Fraction 5	133
Fraction 6	172
Fraction 7	180

Table 3 Maxima of the energy barrier distributions of the investigated samples in the available temperature range

| Sample	E^{max} (K)
Original solution	194
Fraction 1	92
Fraction 2	150
Fraction 3	190
Fraction 4	225

Fig. 2 Energy barriers versus temperature curve. The temperature data are the maxima of the curves

the iron parts of the solution in relation to the hydrodynamic diameter.

The maximum of the graph, which has been weighted according to the iron quota, is at 107 nm. This is near the hydrodynamic diameter of the initial solution (102 nm). Therefore, the fractions are a rather exact reproduction of the initial solution. Furthermore, this result proves the measurement system works generally.

Results of the TMRX measurements

Four fractions and the original solution show a maximum of the energy barrier distribution in the available temperature range (see Fig. 2). For three of the fractions, which should have the largest core diameter according to the method of fractioning, one cannot make a statement regarding the actual core

diameter. This is because these fractions do not possess a maximum of the energy barrier distribution within the available measurement range between 4.2 K and room temperature. Furthermore all fractions show a maximum at 18 K which is not the result of a Néel relaxation process. This effect will be discussed separately.

Table 3 shows the obtained temperatures for the E^{max} of the original solution and four fractions.

Calculation of core diameters

To calculate a corresponding particle size to the obtained maxima of the energy barrier distributions it is necessary to measure hysteresis loops at different temperatures for each sample that has such a maximum in the available temperature range. The data for $M_R(5K)/M_{0.3T}$ are generally ≤0.5 (see Fig. 3), therefore we can conclude that the resulting anisotropy has a uniaxial character (Stoner and Wohlfarth 1948; Blums et al. 1997).
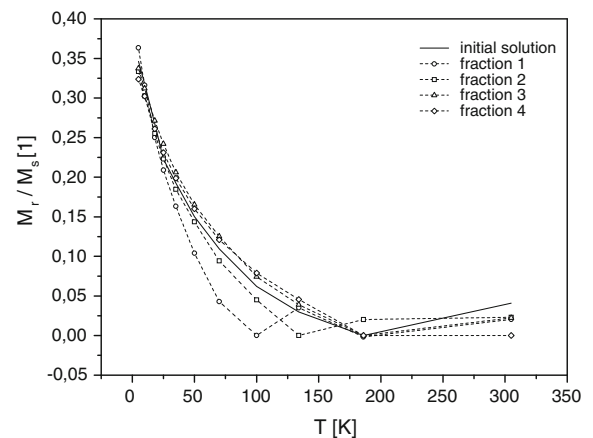
**Fig. 3** Ratio $M_R(5K)/M_{0.3T}$ over the course of temperature

For the determination of H_C independent of the superparamagnetic behaviour of the particles we used the relation

$$\frac{H_C}{H_C^0} = 1 - \left(\frac{T}{T_B}\right)^{\frac{1}{2}}. \tag{8}$$

T_B is the so-called blocking temperature; $T_B \approx 20\frac{KV}{k_B}$. Figure 4 shows the dependence $H_C(T^{1/2})$. By extrapolation to 0 K we get the values H_C^0 (see Table 4). Using the data for H_C^0 and assuming a value of 76 emu/g as saturation magnetization for maghemite at 0 K and a value of 98 emu/g as saturation magnetization for magnetite at 0 K (Bate and Wohlfahrt 1980) we get the data for a weighted K_0 as shown in Table 5.

The results show an increasing anisotropy density for smaller particles, which is in agreement with other investigations (Hanson et al. 1995).

When using (Buschow and De Boer 2003) $V_{max} = \frac{20k_BT}{K}$, where 20 is a factor for the magnetization time τ_{mag}, one can obtain the respective particle volumes and particle diameters at the maxima of the energy barrier distribution (see Table 6).
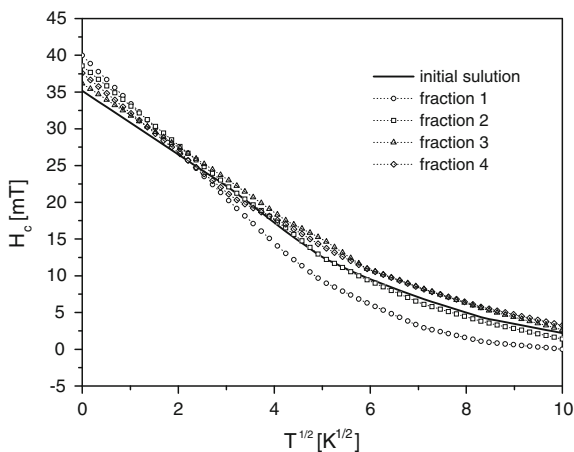
Fig. 4 Coercive field extrapolated to 0 over $\sqrt{T}$

Table 4 Calculated coercive fields at 0 K

Sample	H_C at 0 K (kA/m)
Initial solution	27.9
Fraction 1	31.8
Fraction 2	27.9
Fraction 3	30.2
Fraction 4	28.6

Table 5 Weighted K_0 of the investigated samples

Sample	K_0 (kJ/m³)
Initial solution	12.0
Fraction 1	13.7
Fraction 2	12.0
Fraction 3	13.0
Fraction 4	12.3

Consideration of the temperature dependency of the anisotropy

So far the anisotropy K has been accepted as constant. However, K changes with the temperature and is proportional to the square of the saturation magnetization ($K \sim \beta \cdot M_S^2$), provided that K is affected by the shape anisotropy (Blums et al. 1997). The influence of the $K(T)$ dependence was investigated, e.g., for Fe_XPt_{1-X} particles (Antoniak et al. 2005). To determine the factor of proportionality and, respectively, the factor of demagnetization β, one squares the values of the saturation magnetization which have been obtained through measurement over the temperature course. After that, these values are scaled to the value at 5 K (see Fig. 5).

From the obtained graphs, it is possible to read the factor of proportionality for each sample at the temperature of the maximum of the energy barrier distribution.

From that one can extrapolate $K(T)$, which takes the temperature dependency into account:

$$K(T) = K \cdot \beta. \tag{9}$$

As the samples have at different temperatures a maximum of the energy barrier distribution, each sample has a different anisotropy. Thus, also V_{max} and the diameters change, respectively (see Table 6). If one takes the temperature dependency of the anisotropy into account, the calculated particle diameter increases with temperature (see Table 6).

The results of the measurements of the energy barrier distribution of the different fractions provide clear indication for the success of the fractioning regarding the separation of particles according to their magnetic moment. A decrease of the fractionation current leads to a shift oft the maxima of the energy barrier distributions to higher temperatures of the samples. The differences of the calculated core diameters of the particles support this thesis.

Table 6 Calculated particle diameters of the relevant samples without ($d_{\max,K}$) and with ($d_{\max,K(T)}$) consideration of the temperature dependence of the anisotropy and factor of correction
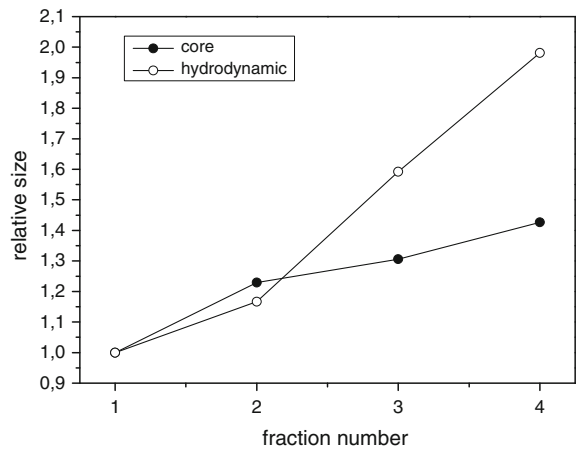
Sample	Max $\rho(E)$ (K)	$d_{\max,K}$ (nm)	Factor of correction β	$K(T)$ (kJ/m^3)	$d_{\max,K(T)}$ (nm)
Initial solution	194	20.4	0.883	10.6	21.3
Fraction 1	92	15.2	0.917	12.6	15.7
Fraction 2	150	18.8	0.915	11.0	19.3
Fraction 3	190	19.8	0.894	11.6	20.5
Fraction 4	225	21.3	0.855	10.5	22.4
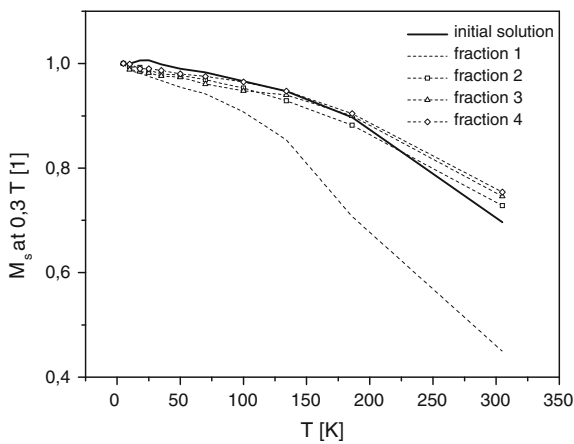
Fig. 5 Scaled *squares* of the saturation magnetization at 0.3 T of the relevant samples

Fig. 6 Relative core sizes and relative hydrodynamic sizes of the four relevant fractions

Comparison of the magnetic active core sizes and the hydrodynamic diameters

Figure 6 shows a comparison of the relative sizes of the relevant fractions calculated from the obtained measurement results using the TMRX method and the MORFF method. The values of the fractions were scaled to the values of fraction 1 for results obtained with both methods. The hydrodynamic size of particles is closely connected to the core size of the particles. A moderate rise of the core size leads to a sharp rise of the hydrodynamic size. While the core sizes increase slightly the hydrodynamic size increases disproportionately high. This process may be influenced by the properties of the used CMD shell (Wagner et al. 2004; Moore et al. 1997). The size of this shell is the determinant factor for the hydrodynamic size. A known fact is the existence of particle size distributions (Hergt et al. 2004). Another possible explanation for the experimental obtained results

can be found in the measurement procedures or in the samples preparation itself. The samples for the TMRX measurements are stable due to the lyophilization process. MORFF is performed in a liquid environment, and accordingly, MORFF determines the hydrodynamic diameter of the nanoparticles, that is, the core together with the hydrated shell. In contrast to the dry-frozen samples the nanoparticles in the liquid MORFF samples can show agglomeration or ageing processes. Buescher et al. (2004) report a lot of possible processes how the particle sizes can vary due to the agglomeration of coated nanoparticles. They have found—in consistence with our findings—a similar correlation between core size and overall particle size in a fractioned ferrofluid with a CMD shell.

Different agglomeration effects can lead to the sharp rise of the hydrodynamic size. As we focused on a comparison between magnetically active and

hydrodynamic sizes in this work, further microscopic measurements would not lead to an additional gain in knowledge, since these would provide details about the overall core size, that is, magnetically active volume plus magnetic dead layer.

Possible explanations for the effect at 18 K

In a previous work Schmidl et al. (2007) also report measured magnetic relaxation processes in this temperature range for a ferrofluid with a similar chemical composition. The existence of small particles can be discarded. In normal cases energy barrier distributions show a lognormal distribution. The peak at 18 K would lead to particle diameters without any size distribution. Moreover, all fractions show this peak. This means the magnetic fractionation does not influence the effect. There are already several explanations for magnetic effects in this temperature area. By using the method of the magnetic after-effects, Kronmüller and Walz (1980) also found relaxation processes at the measured temperature at 18 K in magnetite. They explain those findings with tunnel processes of electrons on domain walls. However, this explanation can be discarded in our case as the examined nanoparticles are particles without domain walls due to their nature as single-domain particles (Blums et al. 1997). So far the explanations found by Kronmüller and Walz are not applicable. Another and possible explanation can be found in surface effects. Fiorani (2005) reports a lot of theoretical and experimental meditations of MNP with their special adverse surface to volume ratio. An important point of view is the magnetically highly frustrated surface area. Effects based on interactions of the magnetic moments (the so-called superspins) of the particles are improbable. On the one hand the strong interaction of the superspins of the particles can be negated in our case based on the preparation process. On the other hand theoretical calculations of Berkov show another behaviour of energy barrier distribution in case of interacting superspins (Berkov 1998). Suzuki et al. (2009) and Sasaki et al. (2005) also investigated non-interacting particle systems with a superparamagnetic behaviour and reported ageing and memory effects at low temperatures using an FC-procedure. This memory effect of the superspins could be a possible explanation of the found relaxation signals at 18 K using the TMRX method.

Conclusions

The success of the magnetic fractionation method has been confirmed using the TMRX and MORFF methods. In agreement with, from other investigations, known behaviour the particle sizes increase with a decreasing fractionation coil current (Romanus et al. 2007; Buescher et al. 2004). The core diameters of every relevant fraction were calculated using the coercive fields H_C^0 and exact anisotropy under consideration of the temperature dependence of the anisotropy. In agreement with other investigations (Hanson et al. 1995; Jeong et al. 2004) the obtained results illustrate an increasing anisotropy density for smaller particles. The comparison of the obtained magnetically active core diameters and the hydrodynamic diameters show a direct relation. With an increase of the magnetic active core diameters the hydrodynamic diameters increase as well. This behaviour is nearly identical with the correlation between overall core size, that is magnetically active part plus magnetic dead layer, and hydrodynamic size, which can be found in all major literature. For the magnetic relaxation effect measured at low temperatures a possible explanation does exist. For the confirmation of the memory effect further investigation are needed.

References

Antoniak C, Lindner J, Farle M (2005) Magnetic anisotropy and its temperature dependence in iron-rich Fe_XPt_{1-X} nanoparticles. Europhys Lett 70:250–256

Bate G, Wohlfahrt EP (1980) Recording materials. In: Handbook of ferromagnetic materials. Elsevier, Amsterdam

Berkov DV (1998) Evaluation of the energy barrier distribution in many-particle systems using the path integral approach. J Phys Condens Matter 10(5):L89–L95

Berkov DV, Kötitz R (1996) Irreversible relaxation behaviour of a general class of magnetic systems. J Phys Condens Matter 8:1257–1266

Blums EA, Cebers AO, Maiorov MM (1997) Magnetic fluids. Walter de Gruyter, Berlin

Buescher K, Helm CA, Gross C, Glöckl G, Romanus E (2004) Nanoparticle composition of a ferrofluid and its effects on the magnetic properties. Langumir 20:2435–2444

Buschow KHJ (2005) Concise encyclopedia of magnetic and superconducting materials. Elsevier Science & Technology, Amsterdam

Buschow KHJ, De Boer FR (2003) Physics of magnetism and magnetic materials. Kluwer Academic, New York

Cotton AA, Mouton H (1907) Nouvelle propriété optique (biréfringence magnétique) de certains liquides organiques non colloïdaux. C R Hebd Seances Acad Sci 145:231–291

Fiorani D (2005) Surface effects in magnetic nanoparticles. Springer, Berlin

Hanson M, Johansson C, Pedersen MS, Morup S (1995) The influence of particle size and interactions on the magnetization and susceptibility of nanometre-size particles. J Phys Condens Matter 7:9269–9277

Hergt R, Hiergeist R, Hilger I, Kaiser WA, Lapatnikov Y, Margel S, Richter U (2004) Maghemite nanoparticles with very high AC-losses for application in RF-magnetic hyperthermia. J Magn Magn Mater 270:345–357

Jeong JR, Lee SJ, Kim JD, Shin SC (2004) Magnetic properties of γ-Fe_2O_3 nanoparticles made by coprecipitation method. Phys Status Solidi B 241:1593–1596

Kronmüller H, Walz F (1980) Magnetic after effects in Fe_3O_4 and vacancy-doped magnetite. Philos Mag B 42(3): 433–452

Moore A, Weissleder R, Bogdanov A (1997) Uptake of dextran-coated monocrystalline iron oxides in tumor cells and macrophages. J Magn Reson Imaging 7:1140

Perrin F (1934) Mouvement brownien d'un ellipsoide—I Dispersion diélectrique pour des molécules ellipsoidales. J Phys Radium 5(10):497–511

Romanus E, Groß C, Kötitz R, Prass S, Lange J, Weber P, Weitschies W (2001) Monitoring of biological binding reactions by magneto-optical relaxation measurements. Magnetohydrodynamics 37:328

Romanus E, Groß C, Glöckl G, Weber P, Weitschies W (2002) Determination of biological binding reactions by field-induced birefringence measurements. J Magn Magn Mater 252:384–386

Romanus E, Berkov DV, Prass S, Groß C, Weitschies W, Weber P (2003) Determination of energy barrier distributions of magnetic nanoparticles by temperature dependent magnetorelaxometry. Nanotechnology 14:1251–1254

Romanus E, Koettig T, Glöckl G, Prass S, Schmidl F, Heinrich J, Gopinadhan G, Berkov DV, Helm CA, Weitschies W, Weber P, Seidel P (2007) Energy barrier distributions of maghemite nanoparticles. Nanotechnology 18:115709

Sasaki M, Jönsson PE, Takayama H (2005) Aging and memory effects in superparamagnets and superspin glasses. Phys Rev B 71:104405

Schmidl F, Weber P, Koettig T, Büttner M, Prass S, Becker C, Mans M, Heinrich J, Röder M, Wagner K, Berkov DV, Görnert P, Glöckl G, Weitschies W, Seidel P (2007) Characterization of energy barrier distribution of lyophilized ferrofluids by magnetic relaxation measurements. J Magn Magn Mater 311:171–175

Stoner EC, Wohlfarth EP (1948) A mechanism of magnetic hysteresis in heterogeneous alloys. Philos Trans R Soc Lond A 240(826):599–642

Suzuki M, Fullem SI, Suzuki IS (2009) Observation of superspin-glass behaviour in Fe_3O_4 nanoparticles. Phys Rev B 79:024418

Wagner K, Kautz A, Röder M, Schwalbe M, Pachmann K, Clement JH, Schnabelrauch M (2004) Synthesis of oligonucleotide-functionalized magnetic nanoparticles and study on their in vitro cell uptake. Appl Organomet Chem 18:514–519